12th International Symposium on Turbulence and Shear Flow Phenomena (TSFP12)
Osaka, Japan, July 19-22, 2022

MECHANICS OF BOUNDARY LAYER TRANSITION INDUCED BY MULTIPLE DISCRETE ROUGHNESS ELEMENTS

Saikishan Suryanarayanan and David B. Goldstein
Department of Aerospace Engineering and Engineering Mechanics
The University of Texas at Austin
Austin, TX 78712.
saikishan.suryanarayanan@gmail.com   david@oden.utexas.edu

Edward B. White
Department of Aerospace Engineering
Texas A&M University
College Station, TX 77840.
ebw@tamu.edu

Garry L. Brown
Department of Mechanical and Aerospace Engineering
Princeton University
Princeton, NJ 08544.
glb1873@msn.com

ABSTRACT
The mechanisms of boundary layer transition caused by multiple discrete roughness elements, as well as by a distributed roughness patch, are studied using immersed boundary direct numerical simulations. The objective is to obtain a broad understanding of how discrete roughness elements can affect the flow around and downstream of neighboring roughness elements, with the aim of extending our mechanistic understanding and mitigation strategies for isolated-roughness-induced transition to a dense array of discrete roughness elements, and possibly distributed roughness. The results are analyzed from instability and vorticity points of view.

INTRODUCTION
Modeling and mitigation of roughness induced transition is a fundamental problem that is relevant for improving the operational efficiency of aircraft (Cebeci *et al.* 1987, Bragg & Gregorek 1989) and wind turbines (Corten & Veldkamp, 2001) that are subject to the environmental accumulation of leading-edge debris.

There has been significant recent progress in understanding roughness induced transition caused by isolated discrete roughness elements (Iyer & Mahesh 2013, Loiseau *et al.* 2014, Suryanarayanan *et al.* 2017). Suryanarayanan *et al*. (2019) identified four different stages in the transition process and provided a vorticity point of view explanation for the mechanisms. The result is summarized in Fig. 1A. Vortical disturbances are generated by the interaction of the incoming boundary layer with the discrete roughness element in the first stage near field of the roughness element. These disturbances are transiently amplified by the lift-up effect in Stage II. The lifted-up structure undergoes a secondary, modal instability in Stage III. This is followed by the ‘breakdown’ to turbulence, increased wall shear stress via counter gradient transport of the mean vorticity and spreading of the turbulent wedge. This understanding has been extended to pressure gradient boundary layers (Suryanarayanan et al, 2020a).

An outcome of this understanding has been in the development of transition mitigation strategies such as roughness shielding (Kuester *et al.*, 2014, Suryanarayanan *et al.*, 2020b). The shielding strategy involves placement of low amplitude distributed roughness or control strips upstream and/or downstream of the large discrete roughness element. The downstream strips were shown to disrupt the streamwise vortices and thus the transition mechanisms.

In order to investigate the practical applicability of roughness shielding and other roughness induced transition mitigation strategies beyond isolated discrete roughness elements, a detailed understanding of interaction of the flow around and downstream of multiple roughness elements is required. This paper therefore aims to extend the vorticity dynamics viewpoint of transition caused by an isolated discrete roughness element (Suryanarayanan *et al.*, 2019) to more realistic situations where there are several discrete roughness elements as well as for a sandpaper inspired distributed roughness strip, to enable the development of suitable transition mitigation strategies and the eventual design of transition resistant surfaces to be used in conjunction with laminar flow airfoils.

The objectives of the paper are to understand

(1) How is the generation of vortical disturbances downstream of a given roughness element affected by the presence of a neighboring roughness?
(2) Is there a wave interaction or coupling between the secondary (modal) instability of neighboring DRE wakes? Specifically, can an unstable DRE wake ‘infect’ otherwise stable DRE wakes in its neighborhood?
(3) What is the effectiveness of shielding strips in a multiple DRE situation? Can shielding the most

dangerous disturbance ensure that nearby subcritical DREs remain stable?

(4) Can this understanding be extended to a random roughness trip?

To answer the above questions, a series of direct numerical simulations involving combinations of marginally supercritical and marginally subcritical DREs and control strips are performed and analyzed.

COMPUTATIONAL METHOD

An immersed boundary, pseudo spectral solver (Goldstein *et al.* 1993, 1995) is used for the direct numerical simulations in this work. This solver is based on the channel flow algorithm of Kim *et al.* 1987.

There is a buffer zone upstream of the useful computational domain that acts as a flow straightener and inflow generator – any steady and unsteady disturbances in the outflow are removed in the buffer zone which forces the flow to be a steady Blasius profile of a specified thickness. There is a virtual wall near the top of the channel that enforces the vertical velocity of a growing Blasius boundary layer. The combination of the buffer zone and the suction wall ensure a near zero-pressure gradient Blasius boundary layer is developed within the useful part of the computational domain in an undisturbed setting. The discrete roughness elements and control strips are created on the bottom surface using immersed boundary forces. This setup is described in detail in Suryanarayanan et al. (2019, 2020b)

This code has been used for boundary layer transition studies with discrete (Sharma *et al.* 2014, Suryanarayanan *et al.* 2019) and distributed roughness (Kuester *et al.* 2014), examination of turbulent wedge evolution (Goldstein *et al.* 2017) and turbulent spots over riblets (Strand, 2007). Many of these studies include favorable comparisons with stability theory, matched water tunnel (Suryanarayanan *et al.* 2019) and wind tunnel experiments (Berger *et al.*, 2017, Suryanarayanan *et al*. 2020b).

The present work uses the same discrete roughness element, inflow conditions and computational domain used in previous studies (Suryanarayanan *et al.* 2020a, 2020b) as the baseline case. The roughness element has a nominal $k^+ = ku_\tau/\nu = 15.15$ and the Reynolds number based on the boundary layer displacement thickness at the roughness location (δ^*_0) is approximately 1480. All the simulations presented in this paper are carried out using 768 × 128 × 192 grid points over a domain of 164.4 δ^*_0 × 8.22 δ^*_0 × 20.6 δ^*_0 in the streamwise, wall-normal and spanwise directions.

RESULTS AND DISCUSSION

Interaction between neighboring DREs

Direct numerical simulations of seven different configurations involving one or more discrete roughness elements are performed in this work. All the simulations have the same computational setup and inflow conditions.

Representative instantaneous snapshots (taken after the simulations have reached a statistically steady state) are shown in Figure 1. Plotted in each figure are an isosurface of streamwise velocity at $U = 0.29\ U_\infty$ colored by streamwise vorticity ω_x. Also shown are isolines of U and contours of ω_x at a cut plane taken at $x/k_1 = 20.6$ from the trailing edge of DRE1. These snapshots thus provide information on the approximate transition location and the shape of the wake and strength of vorticity field downstream of the roughness element(s).

Fig 1(A) shows the roughness induced transition caused by a single serrated DRE with $k_1^+ = 15.15$ discussed in Suryanarayanan *et al*. (2019). In all the other cases, the size and location of this DRE (DRE1) remain fixed. It is of interest to examine whether this DRE can cause nearby subcritical DREs (i.e. ones that would have otherwise been stable in an isolated setting) to transition. Therefore, a second DRE (DRE2) with the same planform but with a smaller height $k_2 = 0.825\ k_1$ is considered. Figure 1B shows the case with DRE2 alone, and it can be observed that it does not cause the flow to transition. This is consistent with observations on the critical value of $k^+ \sim 14$ from previous work on this DRE shape.

It can be observed from Fig. 1C that the tall DRE1 can cause the otherwise subcritical DRE2 nearby to transition. This is because of two main reasons. The proximity between the DREs affects the overall flow field, which can change the "receptivity" of the shorter DRE. This can be better observed in Fig. 1D which has two identical shorter DREs; the strength of the streamwise vortices behind the two are different. The second reason is that the secondary modal instability of the taller DRE1 disturbs the wake of the smaller DRE2 (which would have been stable if the background was quiet).

To separate the two effects, a configuration in which the DREs are staggered such that there is not a significant effect on the receptivity by DRE1 upon DRE2 is considered as case F. The result for this case is broadly similar to Fig. 1C; the wake of DRE2 is disturbed by the unsteady wake of DRE1. There are some differences, however, on the detailed mechanisms, as the wake of the DRE2 is forced by the nearly unimodal Stage III of DRE1 in case C whereas it is excited by the turbulent wedge (Stage IV) in case F. To further analyze this situation, time averaged statistics for mean and fluctuating streamwise velocity are compared for cases A, C and F in Figure 2.

Shown in Fig. 2 are contours of wall shear stress with several stream-normal planes with isolines of mean U and contours of u'_{RMS}. Also shown are streamlines computed from the time averaged velocity field. It can be observed from Fig. 2A1 (Case C) that the shape of the u'_{RMS} contours are similar for both DRE1 and DRE2.

In our previous work (Berger *et al.* 2017) the wake behind the single DRE was examined in wind tunnel experiments and analyzed using linear stability theory (LST). The fluctuations within the wake have three distinct peaks, one at the top of the lifted-up structure (i.e. low-speed streak) and one each at either side. The highest intensity occurred at the top, suggesting that the local 'shear layer' at the top of the low-speed streak was the driver of this instability, what we observe to dominate in both cases A, as well as the wakes of both DREs in case C (see Figs. 2B1 and 2B2).

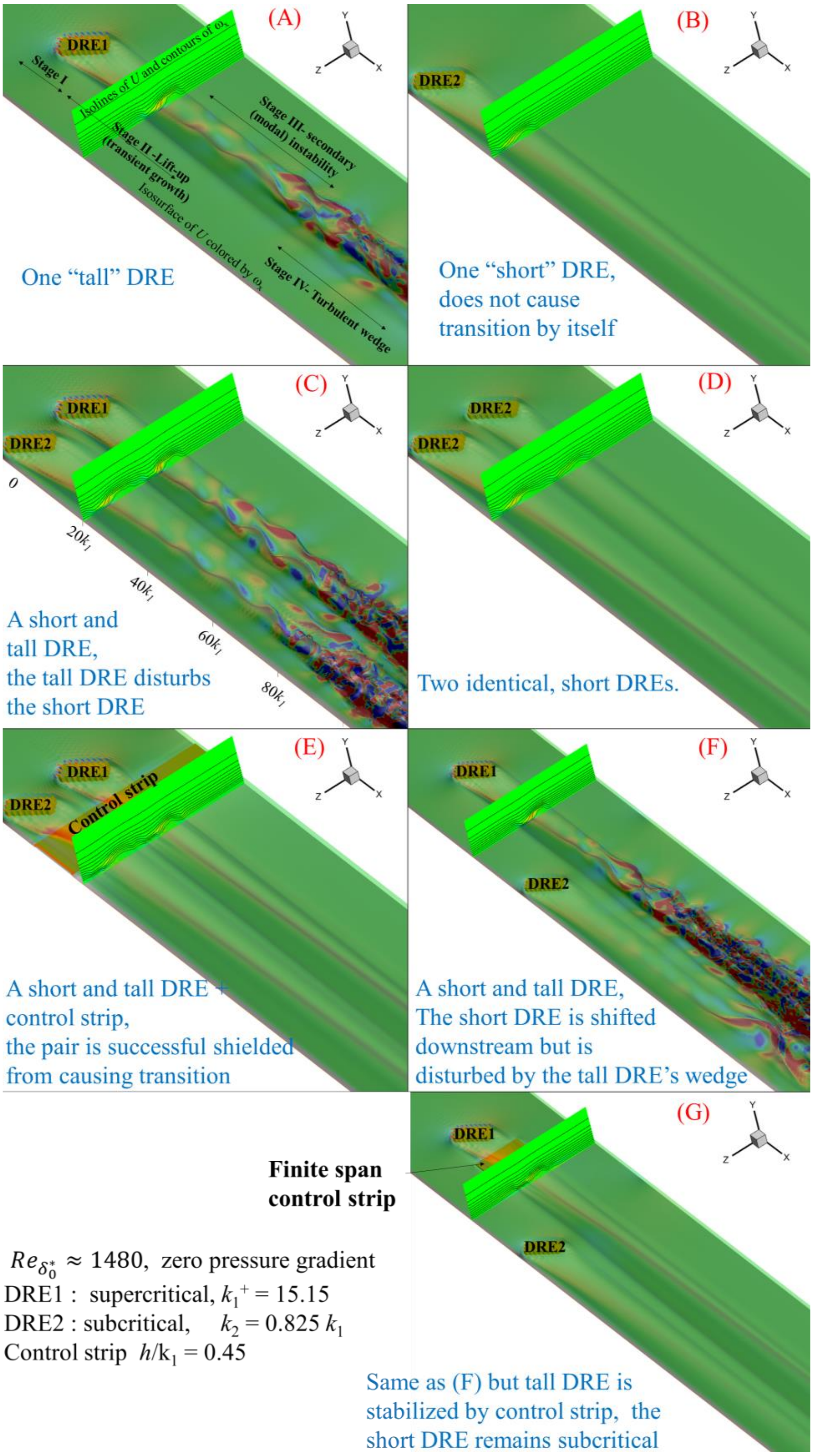

$Re_{\delta_0^*} \approx 1480$, zero pressure gradient
DRE1 : supercritical, $k_1^+ = 15.15$
DRE2 : subcritical, $k_2 = 0.825\, k_1$
Control strip $h/\mathrm{k}_1 = 0.45$

Figure 1: Instantaneous snapshots of the different DNS cases (A-G). The DREs (and control strips) are shown in orange. Plotted in each case are an isosurface of U colored by ω_x and contours of ω_x and isolines of U in stream-normal planes downstream of the DRE(s).

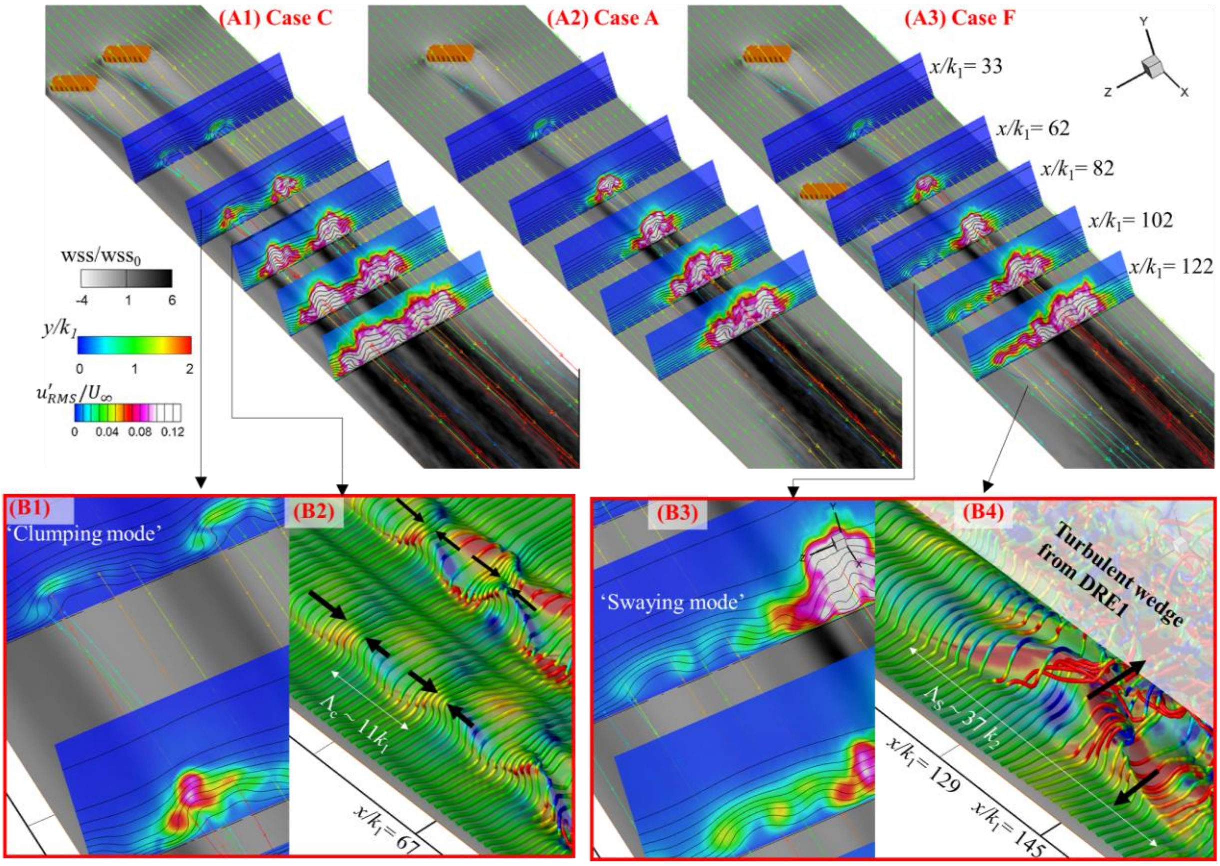

Figure 2: (A1- A3) Time averaged wall shear stress, streamlines (colored by altitude) and contours of u'_{RMS} and isolines of $\overline{U}$ shown in stream-normal planes for cases C, A and F. B1 and B3 zoomed in view of the same data in A1 and A3 showing the clumping mode and swaying mode occurring in the wakes of DRE2 in cases C and F. B2 and B4 show the instantaneous snapshots with vortex lines (colored by ω_x) for cases C and F to provide a mechanistic description of the two modes.

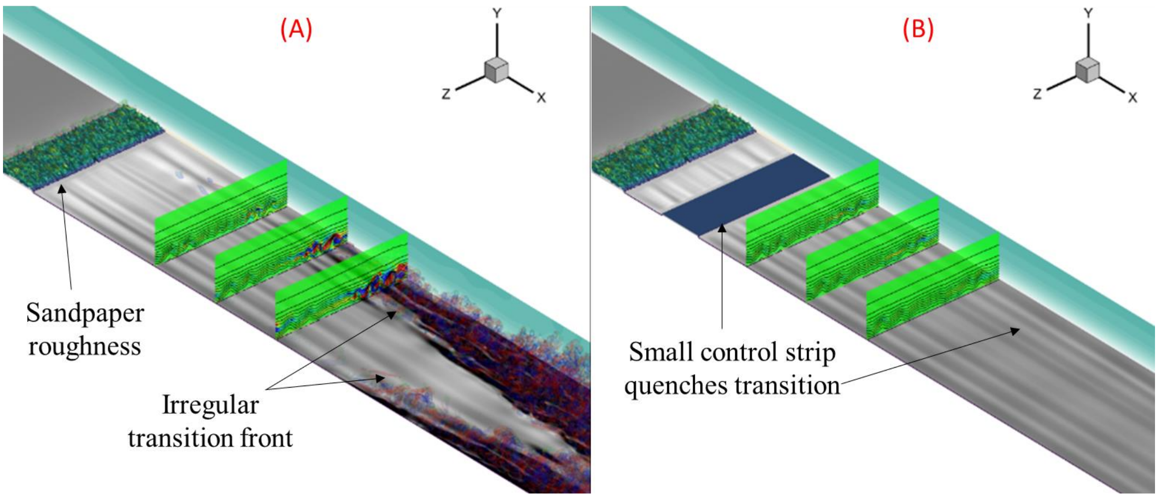

Figure 3. A Transition caused by a sandpaper-like distributed roughness trip. B. Mitigation using downstream shielding by a low amplitude control strip.

From a vorticity point of view, this instability mode driven by the top shear (ω_z) layer can be interpreted as the clumping of the heads of the vortex lines that ride on top of the lifted-up 3D structure, and this leads to tilting of the legs (ω_y) generating an unsteady ω_x. This clumping mode can be clearly observed in Fig. 2B1 and is illustrated using vortex lines in Fig. 2B2 (highlighted with black arrows).

Linear stability analysis (Berger *et al.*, 2017) also showed that there is another, longer wavelength (low frequency) instability that appears with peaks on either side of the lifted-up structure. Band pass filtering of the experimental data confirmed the existence of this low-frequency 'swaying' mode which can be interpreted as being driven by the side (ω_y) shear layers.

Interestingly the wake of DRE2 in case F seems to be dominated by this swaying mode, as observed in Fig. 2B4. While both large and small scale vortical structures exist within the turbulent wedge, it's influence on the velocity field outside the wedge is dominated by the lower frequency - the flow field at the edge of turbulent wedges are known to be dominated by large pancakes of ω_x (see Goldstein *et al.,* 2017). This is also consistent with the hot-wire spectra observed well outside the DRE wake by Berger *et al.* (2017). This swaying mode can be understood from a vorticity point of view as the generation of unsteady ω_x, but this process is not driven by the clumping of the heads and the associated tilting of legs but rather by the spanwise swaying motion of the structure as a whole. This results in a longer wavelength of the instability (nearly 4 times that of the clumping mode), consistent with the findings of Berger *et al.* (2017) for a bandpass filtered single DRE dataset.

Transition control by shielding

Regardless of the detailed mode in Stage III, the broad picture of RIT by multiple DREs remains consistent with the findings for the single DRE. Streamwise vortices generated on the interaction of the DRE(s) with the boundary layer lift-up the background ω_z to generate ω_y (i.e. transient growth of the amplitude of low-speed streaks) which subsequently are subject to a secondary instability. The main differences are that the receptivity of the DRE can be altered by other DREs in their proximity and that stable DRE wakes can be forced by the unsteadiness present in the wakes of transitioning DREs present nearby.

Since the mechanism of transition in a multiple DRE system is still dominated by the lift-up caused by streamwise vortices, the same control schemes may be expected to work. A downstream control strip of height $0.45k_1$ and chord $12k_1$ placed about $5k_1$ behind the DRE pair (E) prevents transition. The peak value of ω_x/ω_{z0} (where ω_{z_0} is the vorticity at the wall of the undisturbed laminar boundary layer at the location of DRE1) in a plane 20.6 k downstream of the DREs (as observed in the instantaneous snapshots) is significantly reduced for both the DREs by the control strip. For DRE1 the value of ω_x/ω_{z0} decreases from 0.37 to 0.20 and in the wake of DRE2 the streamwise vorticity is reduced from 0.33 to 0.16, thus rendering both of them subcritical. There is likely to be some temporal variation in these precise numbers for the unsteady cases, but the strips appear to approximately cause a 50% reduction in the streamwise vorticity magnitude. The mechanism by which the strips work, and a theoretical model are described in Suryanarayanan at al. (2020b) and (2020c) respectively.

Case F, in which DRE2 is placed downstream and transitions only because of the unsteady forcing of the wedge, presents an interesting case for studying control. Case G considers just suppressing the transition behind the larger DRE1 by disrupting it's streamwise vortex with a *finite span* control strip. In this case, the control strip by itself does not directly affect the flow around DRE2; and any effect observed on the wake of DRE2 is primarily due to the change in the wake of DRE1. The control strip reduces the peak ω_x to 0.19 from a value of 0.34 for the isolated DRE case, preventing DRE1's transition. It can be observed that disrupting the larger DRE1's transition in this case, can prevent the smaller DRE2 from transitioning too, as the modal disturbances that excite its wake are no longer present. If we quench the unsteady disturbances soon enough, we may be able to keep them from 'infecting' nearby subcritical wakes.

Extension to distributed roughness

The next step is to extend these results to the distributed roughness case. While discrete and distributed roughness have been treated separately in literature, our studies (Suryanarayanan *et al.,* 2021, *manuscript under preparation*) show that there is similarity in the late-stage transition processes that increase wall shear stress across both discrete and distributed roughness induced transition. In this paper, we consider a 'sandpaper' like distributed roughness trip in Fig. 3. Preliminary results show similar mechanisms at play not just in the final stages, but throughout the transition process, at least for this specific distributed roughness considered here –

(a) Generation of streamwise vortices by the interaction of the roughness with the incoming boundary layer
(b) Lift-up and transient amplification
(c) The most dangerous disturbances undergo modal instability, and these may excite subcritical wakes in their neighborhood.

A detailed analysis of this case will be presented elsewhere, but Fig. 3B shows that shielding strips can delay transition downstream of distributed roughness as well by reducing the magnitude of streamwise vortices, supporting the broad similarity of mechanisms. We note however, that random roughness strips can cause receptivity to Tollmien–Schlichting waves that can eventually cause classical transition and the role of the strips or other surface textures on mitigation of classical transition is yet to be studied.

CONCLUDING REMARKS

The series of direct numerical simulations presented in this paper helps extend the mechanistic understanding of boundary layer transition caused by an isolated discrete roughness element to situations involving multiple discrete roughness elements, as well as to certain classes of distributed roughness. The results show that DREs can affect the flow field around other DREs in close proximity and thus alter the vortical disturbances generated in their wakes. Even if the DREs are not close enough to affect the nearfield flow, a transitioning DRE wake can force (or 'infect') otherwise subcritical wakes of neighboring or downstream DREs and cause them to transition. This is particularly significant in real-world situations such as aircraft wing leading edge subject to insect splatter; a single large roughness could potentially cause the flow downstream of many smaller roughness elements around it to transition. For the DRE shapes and configurations considered here, it is found that a transitioning DRE can excite either the clumping mode or the swaying mode of the subcritical DRE. The latter appears to be likely when the subcritical wake is forced by the disturbances at the edge of a nearby turbulent wedge. Control strips are demonstrated to mitigate transition caused by multiple roughness elements. The control strips work by disrupting individual streamwise vortices, and since the lift-up by streamwise vortices continues to be a significant part of the transition process involving multiple DREs, the control strips remain effective. The work also demonstrates that preventing the most dangerous disturbance from transitioning can also prevent it from infecting neighboring subcritical wakes. Preliminary results indicate that much of this understanding and control effectiveness appear to be valid for situations involving distributed roughness such as a sandpaper trip.

ACKNOWLEDGEMENTS

This work is sponsored by the US Air Force Office of Scientific Research through grant# FA9550-19-1-0145. We thank the Texas Advanced Computing Center (TACC) at the University of Texas at Austin for providing High-Performance Computing resources.

REFERENCES

Berger, A.R., McMillan, M.N., White, E.B., Suryanarayanan, S. and Goldstein, D.B., 2017. Suppression of transition behind a discrete roughness element using a downstream element. In *Tenth International Symposium on Turbulence and Shear Flow Phenomena*. Begel House Inc.

Bragg, M. and Gregorek, G., 1989. Environmentally induced surface roughness effects on laminar flow airfoils-Implications for flight safety. In Aircraft Design and Operations Meeting (p. 2049).

Cebeci, T., 1987. Effects of environmentally imposed roughness on airfoil performance. NASA Contractor Report 17963.

Corten, G.P. and Veldkamp, H.F., 2001. Insects can halve wind-turbine power. *Nature*, **412**(6842), pp.41-42.

Goldstein, D.B, Chu, J. and Brown, G.L, 2017. Lateral Spreading Mechanism of a Turbulent Spot and a Turbulent Wedge. *Flow, Turbulence and Combustion*, **98**(1), pp.21-35.

Goldstein, D.B, Handler, R. and Sirovich, L., 1995. Direct numerical simulation of turbulent flow over a modeled riblet covered surface. *Journal of Fluid Mechanics*, **302**, pp.333-376.

Iyer, P.S. and Mahesh, K., 2013. High-speed boundary-layer transition induced by a discrete roughness element. *Journal of Fluid Mechanics*, **729**, pp.524-562.

Kim, J., Moin, P. and Moser, R., 1987. Turbulence statistics in fully developed channel flow at low Reynolds number. *Journal of Fluid Mechanics*, **177**, pp.133-166.

Kuester, M.S., Sharma, A., White, E.B., Goldstein, D.B. and Brown, G., 2014. Distributed Roughness Shielding in a Blasius Boundary Layer. AIAA paper 2014-2888. In *44th AIAA Fluid Dynamics Conference*.

Loiseau, J.C., Robinet, J.C., Cherubini, S. and Leriche, E., 2014. Investigation of the roughness-induced transition: global stability analyses and direct numerical simulations. Journal of Fluid Mechanics, **760**, pp.175-211.

Sharma, A., Drews, S. D., Kuester, M. S., Goldstein, D. B., and White, E. B., 2014, "Evolution of Disturbance due to Discrete and Distributed Surface Roughness in Initially Laminar Boundary Layers," *AIAA* Paper 2014-0235.

Strand, J., 2007. DNS of surface textures to control the growth of turbulent spots. Masters Thesis, The University of Texas at Austin, Dec. 2007.

Suryanarayanan, S., Goldstein, D.B. and Brown, G.L., 2017. Roughness induced transition in wall bounded flow: A vorticity point of view. In *Tenth International Symposium on Turbulence and Shear Flow Phenomena*. Begel House Inc.

Suryanarayanan, S., Goldstein, D.B. and Brown, G.L., 2019. Roughness induced transition: A vorticity point of view. *Physics of Fluids*, **31**(2), p.024101.

Suryanarayanan, S., Goldstein, D.B., Berger, A.R., White, E.B. and Brown, G.L., 2020a. Effect of pressure gradients on the different stages of roughness induced boundary layer transition. *International Journal of Heat and Fluid Flow*, **86**, p.108688.

Suryanarayanan, S., Goldstein, D.B., Berger, A.R., White, E.B. and Brown, G.L., 2020b. Mechanisms of roughness-induced boundary-layer transition control by shielding. *AIAA Journal*, **58**(7), pp.2951-2963.

Suryanarayanan, S., Goldstein, D. and Brown, G., 2020c. Interaction of Streamwise Vortices with Surface Textures–DNS and Analysis. AIAA paper 2020-3020.

Suryanarayanan, S., Goldstein, D. and Brown, G., 2021. Counter-gradient vorticity transport mechanisms in boundary layer transition: Insights from conditional statistics. *Bulletin of the American Physical Society*, **66**.

Xiao, D., Borradaile, H., Choi, K.S., Feng, L., Wang, J. and Mao, X., 2021. Bypass transition in a boundary layer flow induced by plasma actuators. *Journal of Fluid Mechanics*, **929**, A6. doi:10.1017/jfm.2021.835.